Letter

Efficient general waveform catching by a cavity at an absorbing exceptional point

Asaf Farhi,[1] Wei Dai,[1] Seunghwi Kim,[2] Andrea Alù,[2,3] and Douglas Stone[1,4]

[1]*Department of Applied Physics, Yale University, New Haven, Connecticut 06520, USA*
[2]*Photonics Initiative, Advanced Science Research Center, City University of New York, New York, New York 10031, USA*
[3]*Physics Program, Graduate Center, City University of New York, New York, New York 10016, USA*
[4]*Yale Quantum Institute, Yale University, New Haven, Connecticut 06520, USA*

(Received 14 October 2023; accepted 27 March 2024; published 17 April 2024)

We study a system tuned to an absorbing exceptional point and explore its use to efficiently receive and store an incoming wave with an envelope different from the absorbing-eigenmode envelope. Specifically, while absorbing states of lossless resonators have an exponentially increasing envelope, we focus on capturing naturally emitted waves with an exponentially decreasing envelope. We find that, when tuning a cavity to an nth-order absorbing exceptional point (EP), $n+1$ temporal orders of *any* incoming waveform can be perfectly captured, leading to significantly less scattering and increasing the overall absorption efficiency for general waveforms. We present an approach to tune a cavity to an EP and demonstrate less scattering by an order of magnitude for a decaying incoming waveform. Our results may be used for efficient passive state transfer and detection of spontaneous emission.

DOI: 10.1103/PhysRevA.109.L041502

Resonators possess absorbing eigenstates with real or complex eigenfrequencies, which can be determined by solving the boundary-value problem with incoming boundary conditions. When a resonator is excited with such an eigenstate, it exhibits no scattering [1,2]. However, whereas physical systems usually have absorbing eigenfrequencies in the upper complex frequency plane, waves that impinge on a resonator typically do not have the temporal dependence of such eigenstates, resulting in considerable scattering. In this Letter, as opposed to previous works that considered excitations with absorbing eigenstates [1–3], we aim at significantly reducing the scattering for a general temporal profile of the incoming waveform both in lossy and lossless resonators. This is useful for many physical systems, which cannot be engineered to have absorbing eigenfrequencies that match the typical incoming waveforms, such as lossless systems or when the materials required to realize the physical parameters do not exist. While our approach is expected to apply to many fields of physics such as acoustics, elastodynamics, matter waves, and quantum light [4–7], we focus on electromagnetic waves at microwave and optical frequencies, of relevance for classical and quantum technologies.

Photon transfer between cavities is a fundamental process in both classical and quantum networks, and it has been used in quantum computation and communications at microwave and optical frequencies [8–13]. Deterministic protocols based on direct state transfer [14], which achieve large entanglement rates, have recently been realized in superconducting circuit systems featuring "pitch and catch" of microwave photons. In such experiments a resonant cavity coupled to an atom (or artificial atom) is usually utilized as a quantum node [15–17]. Photon detection is another topic of paramount importance in quantum information, and for probing processes such as atomic or molecular spontaneous emission, electron spin resonance, nuclear magnetic resonance, and fluorescence [18–22]. A key requirement for photon detectors is to achieve a large detection efficiency of incoming photons [23]. A common implementation of a photon detector relies on a lossless or lossy resonant cavity [19,20]. Photon detection is usually ineffective at triggering measurable phenomena at microwave frequencies since photons have five orders of magnitude lower energies compared with optical frequencies [24].

The most efficient way to load a lossless resonator is with an input wave at its complex absorbing eigenfrequency, which has an *increasing* exponential waveform [see Fig. 1(b)], the complex frequency generalization of a coherent perfect absorber (CPA) [1,2,15,25–29]. However, for state transfer such a waveform needs to be generated in the pitch process, which results in emission, which may not be compatible with quantum networks [30], and photons emitted in natural processes usually do not have this waveform. Despite the existing techniques of active pulse shaping of flying photons [15,16,31–40], it remains important to passively catch photons that are naturally emitted from cavities or in spontaneous emission [41–43]. Such emitted photons have a *decaying* exponential waveform [see Fig. 1(a)], and when passively caught by a standard receiving cavity, the efficiency is rather poor, of typically only 60% [25]. Clearly, the efficient passive capture of naturally emitted photons holds the potential to allow quantum state transfer to operate at optical frequencies and exceptional detection of processes such as spontaneous emission.

It was recently shown that by designing a cavity to operate at an exceptional point (EP) [44–48] of CPAs, in which CPA eigenvalues and eigenmodes coalesce [49,50], the absorption spectrum on the real-ω axis becomes quartic [49,50]. More recently, the concept of CPA EP was generalized to complex frequencies where two or more complex absorbing eigenfrequencies coalesce (virtual CPA EP) [3,50]. In Ref. [3] the time-domain properties of CPA EPs were studied both for

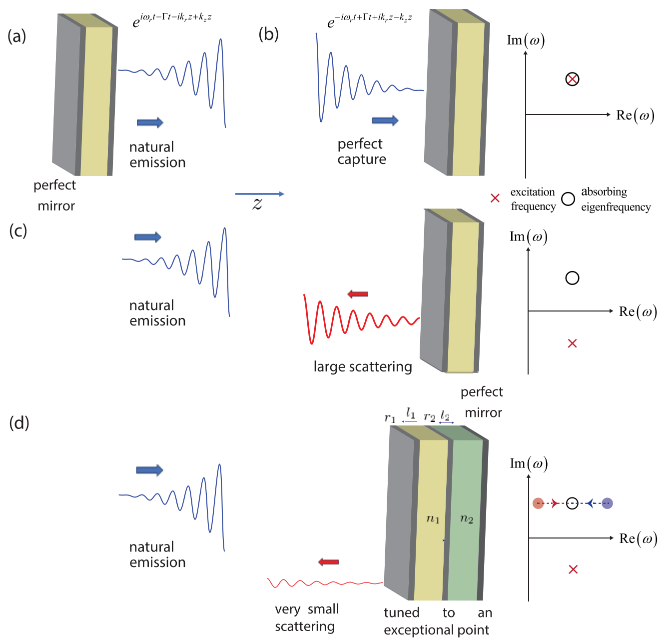

FIG. 1. (a) Naturally emitted waveform from a cavity decays (increases) exponentially in time (space, presented above). Such a waveform is emitted in spontaneous emission by an atom or molecule. (b) A waveform that increases (decays) exponentially in time (space) is perfectly captured by a cavity. Right: The complex excitation frequency (blue circle) and absorbing eigenfrequency (red cross) match. (c) Passive state transfer with standard cavities. Since the naturally emitted and perfectly captured waves do not match, 40% of the incident field is scattered. (d) Passive state transfer with a cavity system tuned to a virtual absorbing exceptional point where two absorbing eigenfrequencies coalesce. Since the EP cavity captures another order in time of the incoming waveform, there is very small scattering.

real and complex ω. It was shown that CPA EPs extend the class of waveforms, which can be perfectly absorbed, namely $E \propto (vt - z)^m e^{i(kz-\omega_r t)+\Gamma t}$, where $\Gamma = 0$ and $\Gamma \neq 0$ for real-ω and virtual CPA EP, respectively, m is the EP order, and the waveforms have a frequency content at a single ω for infinite time pulses [3]. It was demonstrated that these high-order waveforms have dramatically improved performance in wave capturing [3,51]. CPA EP is now understood to be a universal geometry-independent phenomenon in scattering, albeit requiring resonator tuning or design to create a degeneracy of purely incoming eigenfunctions of the wave equation. In the current Letter we only consider the geometry of a one-port resonator tuned to an EP, showing how such a resonator can perform improved wave capture in the time domain. However, all of the temporal behavior we describe will apply to an arbitrary multiport system at CPA EP, as long as the system is excited with the appropriate coherent superposition of incoming channels.

Here, we first show that a cavity at a CPA EP perfectly captures additional orders in time for *any* waveform envelope, enabling efficient capturing of waveforms with general envelopes/amplitude modulations. We then present a semianalytical approach to tune a catching port that is of the type used in quantum information processing to a virtual CPA EP.

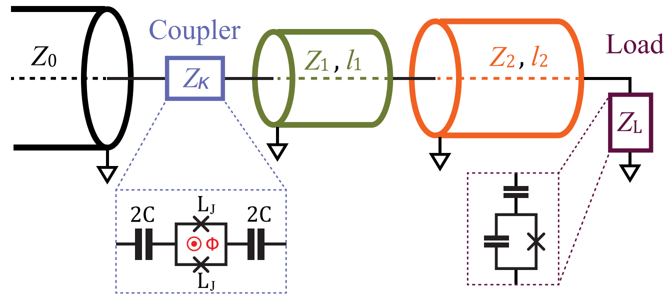

FIG. 2. A schematic of the setup: A flux-controlled coupler and two transmission lines (microwave analog of the optical cavities) loaded by a transmon, tuned to an absorbing virtual exceptional point. The coupler is composed of two capacitors each of capacitance $2C$ and a superconducting quantum interference device (SQUID), which can be modeled by an inductance $L = L_J/\cos(\Phi/\phi_0)$.

We next show that when this system is at an EP, it significantly improves the efficiency in the catch process of the waveforms $e^{i(\omega_r t-kz)+\Gamma t}$, $(vt - z)e^{i(\omega_r t-kz)+\Gamma t}$ and can address additional applications that have been challenging [25]. Finally, we demonstrate that by utilizing such a cavity, the pitch and catch process can be performed without modifying the naturally emitted wave, i.e., passive state transfer, at high efficiency [see Fig. 1(d)] and discuss the advantage for single-photon detection.

We consider a single-port setup composed of two transmission line sessions loaded by a capacitively coupled transmon qubit, and a flux-controlled coupler, which is typical in circuit QED (cQED) experiments (see Fig. 2). For applications at optical frequencies [21] a photon detector and coating layers could replace the transmon and transmission lines, respectively, and for a lossy detector the coupler may not be required. We will now show that a first-order real or complex-ω CPA EP enables the capture of any waveform up to linear order in time. Clearly, waveforms with a significant linear order term will substantially benefit from such an EP. We focus on naturally emitted waveforms which are of practical importance, can have a significant linear term, and their passive catching is somewhat counterintuitive. Let us assume that we do not modulate the coupling in the pitch process and the emitted photon has the form $e^{-\Gamma_2 t+i\omega_r t}$. We consider a cavity at a general complex-ω CPA EP in the catch process with the same ω_r as the emitting cavity but with Γ. Note that the imaginary parts of the frequency of the incoming wave and the absorbing eigenfrequency are different and have an opposite sign, unlike the situation in Ref. [3]. More generally, for a system with an absorbing eigenfrequency of $\omega = \omega_r + i\Gamma$ we analyze here the advantage of an EP in capturing incoming waves of the form $g(t)e^{i\omega_r t}$ for any $g(t)$. At a CPA EP any signal of the form $e^{\Gamma t}(a + bt)$ can be perfectly captured (for any a, b) [3]. We Taylor expand the naturally emitted wave and the above-mentioned form and obtain that there exist a, b for which they are equal to linear order,

$$e^{-\Gamma_2 t} \approx e^{\Gamma t}[1 - (\Gamma + \Gamma_2)t], \tag{1}$$

which means that the naturally emitted wave will be perfectly captured to linear order. Similarly, at an exceptional point with three coalescing eigenmodes and eigenfrequencies, the naturally emitted wave will be perfectly captured up to quadratic order, which implies longer times,

$$e^{-\Gamma_2 t} \approx e^{\Gamma t}\left[1-(\Gamma+\Gamma_2)t+\tfrac{1}{2}(\Gamma+\Gamma_2)^2 t^2\right]. \quad (2)$$

Clearly, this can be generalized to higher-order EPs and any incoming wave envelope. It is important to note that this is a *transient* effect that is valid up to a certain time, which increases with the EP order, as opposed to the cases considered so far of capturing an eigenstate at a CPA or virtual CPA or CPA EP [1–3], which are more efficient for long times. Similarly, one could expand around t_1 (for any t_1), which implies that for long pulses the output that originates from an input at a given time will destructively interfere well with outputs that originate from inputs at adjacent times. Note that the polynomial $a + bt + \cdots$ does not expand the incoming waveform but it expands the function obtained by dividing the incoming wave by $e^{\Gamma_2 t}$. It is also worth mentioning that the analysis above applies to any system that is tuned to an absorbing EP. This greatly enhances the capturing efficiency, as we show below.

We now present an approach to calculate EPs for our setup, which reduces a highly complex calculation that is usually approximate to an eigenvalue equation with a very accurate solution. Note that the previously derived approach in Ref. [3] for calculating EPs is not applicable to the more complicated yet realistic system with the coupler, which we deal with here. We denote the transmission line impedances by Z_1, Z_2 and the characteristic impedance by Z_0 and write the reflection coefficients at the $Z_0 - Z_1$, $Z_1 - Z_2$, and $Z_2 - Z_3$ as follows

$$r_1 = \frac{Z_k(\omega)+Z_1-Z_0}{Z_k(\omega)+Z_1+Z_0}, \quad r_2 = \frac{Z_2-Z_1}{Z_2+Z_1}, \quad r_3 = \frac{Z_L(\omega)-Z_2}{Z_L(\omega)+Z_2},$$

where we include the coupler and load with the impedances $Z_k(\omega)$ and $Z_L(\omega)$ at the $Z_0 - Z_1$ and $Z_2 - Z_3$ interfaces and the transmon load could be modeled by a lumped-element circuit. By imposing boundary conditions, we obtain the total reflection coefficient

$$r = \frac{r_1(\omega)(-r_2 r_3 e^{2ikl_2}+1)+e^{2ikl_1}[r_2 - r_3(\omega)e^{2ikl_2}]}{1-r_2 r_3 e^{2ikl_2}+r_1(\omega)e^{2ikl_1}[r_2-r_3(\omega)e^{2ikl_2}]},$$

where l_1 and l_2 are the lengths of the first and second transmission lines, respectively. Note that transmission lines can be designed with their impedances different while maintaining the same propagation speeds [52]. For simplicity, we set the propagation speed to c.

It has been shown that the conditions for a CPA EP are $r = 0$ and $\frac{dr}{d\omega} = 0$, which correspond to $g = 0$ and $\frac{dg}{d\omega} = 0$, where g represents the numerator of r [3]. Let us first set $g = 0$ to obtain r_2 as follows:

$$r_2 = \frac{r_3(\omega)e^{2ikl_1}e^{2ikl_2} - r_1(\omega)}{e^{2ikl_1} - r_3 r_1(\omega)e^{2ikl_2}}. \quad (3)$$

Since r_2 is real we express from $\mathrm{Im}(r_2) = 0$ a variable, e.g., $Z_1(\omega, r_3(\omega), l_1, l_2, Z_k(\omega))$, which we substitute in r_2 and the equation formed by equating the two expressions for r_2. From this equation we find $Z_2(\omega, r_3(\omega), l_1, l_2, Z_k(\omega))$ and then substitute Z_1, Z_2, and r_2 in $dg/d\omega = 0$ to get the EP equation:

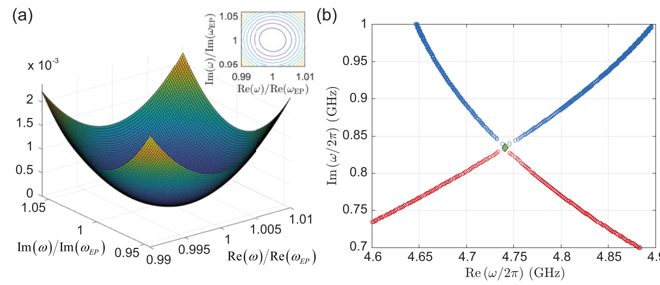

FIG. 3. (a) $|r|$ as a function of $\mathrm{Re}(\omega)$ and $\mathrm{Im}(\omega)$ close to the EP in surface and contour (inset) plots. The scaling is quadratic in two dimensions (2D) as expected since at the EP $|r| \propto (\omega - \omega_n)^2$ and the derivative with respect to a complex variable is equal to the derivatives from all directions, which verifies the calculation of the virtual CPA EP. (b) Coalescence of the eigenfrequencies that satisfy the equation $r = 0$ at the EP when varying l_1/l_2, where the diamond denotes the EP.

$$\frac{dg}{d\omega}(\omega, Z_L(\omega), l_1, l_2, Z_k(\omega)) = 0. \quad (4)$$

Note that the procedure and expressions described above are expected to apply to most catching port implementations.

For concreteness, we assume a linear response, neglecting the nonlinearity from the weakly coupled transmon and the coupler, which is justified for the case of a single photon [53,54]. We also assume that the transmon is decoupled from the transmission lines during the drive [25], which implies $r_3 = -1$. We model the coupler as a lumped LC element (whose inductance is external-flux dependent), with the impedance given by $Z_k = j\frac{\omega^2 LC - 1}{\omega C}$. While the practical schemes to implement the coupler are mostly at the microwave, recent works suggested an analogy between circuit elements and optical components [55–61]. In addition, there was recent progress in optical switching, which can rapidly switch off the coupler [62,63].

We then proceed to derive the analytic EP equation. To that end, we express C from $\mathrm{Im}(r_2) = 0$, fix $\omega_d = 1/\sqrt{LC} = 2\pi \cdot 5$ GHz, and obtain $\frac{dg}{d\omega}(\omega, l_1, l_2, Z_1) = 0$, where we performed the analytical operations described above computationally, see Supplemental Material I (SM) [64] for details. To solve the EP equation semianalytically, we set $Z_0 = 50\ \Omega$ and choose $Z_1 = 100\ \Omega$. We then obtain $\mathrm{Re}(\omega_{\mathrm{EP}}) = 2\pi \cdot 4.727$ GHz, $\mathrm{Im}(\omega_{\mathrm{EP}}) = 2\pi \cdot 0.834$ GHz, $l_1 = 0.0215$ m, $l_2 = 0.0276$ m, $C = 0.3037$ pF, $Z_2 = 60.27\ \Omega$. To verify the EP calculation, we plotted $|r|$ as a function of $\mathrm{Re}(\omega)$ and $\mathrm{Im}(\omega)$ and present it in Fig. 3(a). It can be seen that there is a clear quadratic dependency in two dimensions, for such a dependency on the real-ω axis see Ref. [49]. In Fig. 3(b) we plot the coalescence of absorbing eigenfrequencies at the EP, which demonstrates the remarkable accuracy of our EP calculation.

To quantify the capturing efficiencies of the exponentially increasing and naturally emitted inputs at the virtual CPA EP, we calculated the scattered fields. This calculation was performed using a numerical inverse Fourier transform by definition since our lossless system has real refractive indices and there are no numerical divergences (topics that were addressed

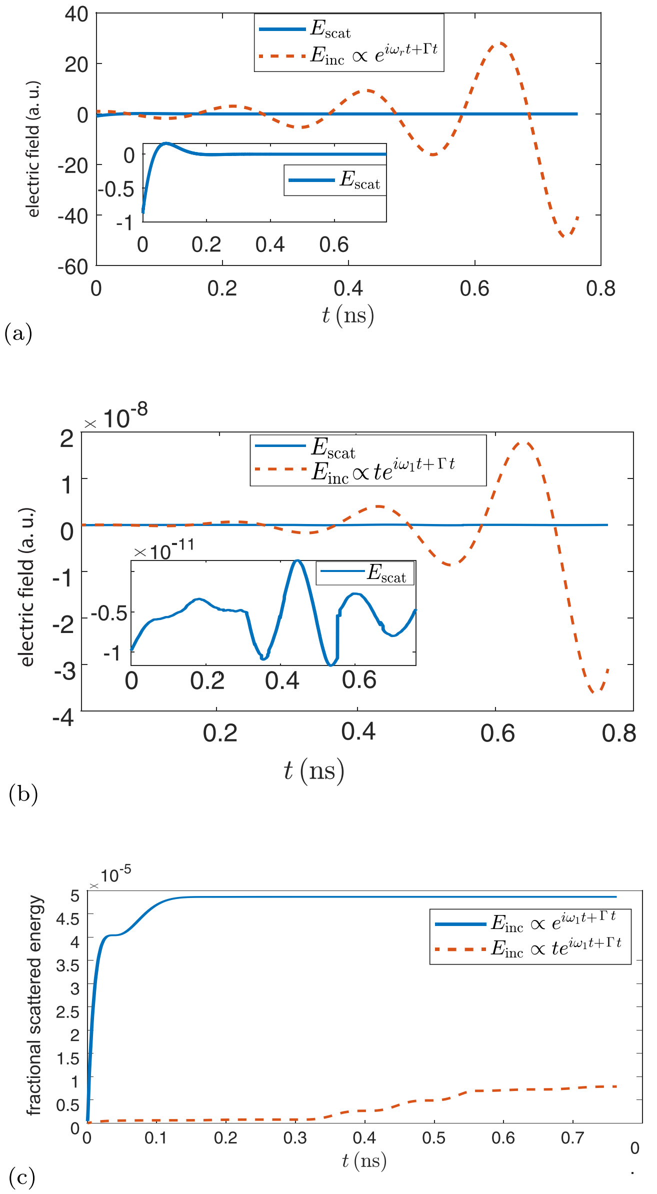

FIG. 4. The incoming and scattered fields as functions of time for the inputs (a) $e^{i\omega t+\Gamma t}$ and (b) $te^{i\omega t+\Gamma t}$. (c) Fractional scattered energy for both incoming fields as functions of time. Note that for the EP parameters, the roundtrip is less than an oscillation period, resulting in rapid equilibration.

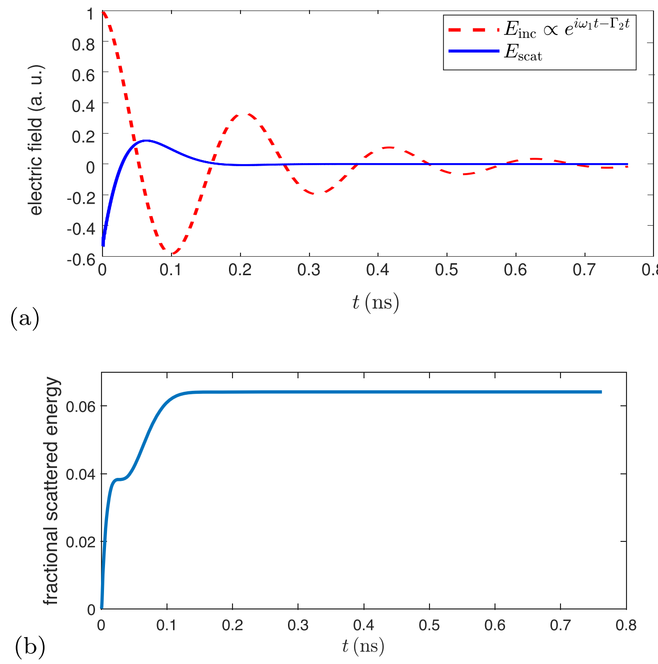

FIG. 5. (a) The incoming and scattered fields as functions of time for the inputs $e^{i\omega t-\Gamma t}$, which show that the naturally emitted wave $e^{i\omega t-\Gamma t}$ is well captured by the CPA EP cavity. (b) Fractional scattered energy as a function of time. Importantly, the efficiency for this passive quantum state transfer is >93%. Note that there are only two or three roundtrips of the incoming wave, and therefore no significant scattering is expected for the input $e^{i\omega t-\Gamma t}$ during the second half since there is a delay between the input and output and the linear approximation holds in the first half.

in Ref. [3]). In Fig. 4 we present the scattered fields and fractional scattered energies $\int_0^t E_{\rm sc}^2 dt'/\int_0^t E_{\rm inc}^2 dt'$ for the exponentially growing inputs $e^{i\omega t+\Gamma t}$ and $te^{i\omega t+\Gamma t}$. The fractional scattered energies are 5×10^{-5} and 10^{-5}, respectively, which outperform the efficiency of 99.4% reported in Ref. [25], and exceed the fidelities required for good logic gates and measurements. In Fig. 5 we present the scattered fields and fractional scattered energies for the naturally emitted wave $e^{i\omega t-\Gamma t}$. Importantly, while the previously reported fractional scattering for such a wave is 39% [25], in our case, it is less than 7%, even though our Q factor is larger by a factor of 2.61, which is expected to reduce the performance (e.g., due to a large r_1). This fractional scattering can be further decreased by reducing the value of r_1. To confirm this we calculated another EP with 1.63 times lower Q factor and obtained 4.5% fractional energy (see SM II [64] for details). We can thus extrapolate that using our approach for the same Q factor a first-order CPA EP will perform approximately an *order of magnitude better*. In SM III [64] we also plot the scattered field for the drive $te^{i\omega t-\Gamma t}$, which has a relatively large scattered field since the system captures only one temporal order of the input. As noted, this process does not require modulation of the coupler, which holds the potential to enable applications at optical frequencies. Similarly, photon detection of waveforms emitted in many processes such as spontaneous emission can be significantly improved. In SM IV [64] we also analyze a setup of a charged coupled device (CCD) with two coating layers, which is relevant for optical frequencies. We tune it to complex and real absorbing EPs, where in the latter case the coupler may not be required.

In summary, we first showed that an absorbing exceptional point captures additional temporal orders of any incoming waveform. We presented a general approach to tune the catching port to an exceptional point, which is valid in the weak- and strong-coupling regimes and achieves a very high calculation accuracy. We then demonstrated that our system performs significantly better compared with the existing approaches in terms of catching efficiency. Specifically, we showed that a virtual CPA EP port can efficiently catch naturally emitted decaying waves, potentially opening avenues for applications at both microwave and optical frequencies, such as distributed quantum computation [10,11], quantum communication [12,13], or reading-out neutral atom qubits [21,22]. Though in our simulation the electromagnetic wave is treated classically, we do not expect decoherence to degrade the efficiency for any nonclassical states encoded in the wave packet for small photon numbers [53,54]. It is important to note that having a large decay rate Γ of the receiving port improves the performance, even if it increases the distance to complex ω of the incoming wave, and requires more rapid temporal control (e.g., switch off) of the incoming wave. It is also worth mentioning that our approach is valid for lossy systems as well, which could be important in certain applications. This general method for enhanced passive wave capture will apply to other fields of physics such as acoustics and matter waves [4–7].

We acknowledge fruitful discussions with V. Joshi, M. Devoret, K. Scheuer, A. Poddubny, and R. Cortinas. This work was partially supported by a grant from the Simons Foundation.

[1] H. Noh, Y. Chong, A. D. Stone, and H. Cao, Perfect coupling of light to surface plasmons by coherent absorption, Phys. Rev. Lett. **108**, 186805 (2012).
[2] D. G. Baranov, A. Krasnok, and A. Alù, Coherent virtual absorption based on complex zero excitation for ideal light capturing, Optica **4**, 1457 (2017).
[3] A. Farhi, A. Mekawy, A. Alù, and D. Stone, Excitation of absorbing exceptional points in the time domain, Phys. Rev. A **106**, L031503 (2022).
[4] A. Müllers, B. Santra, C. Baals, J. Jiang, J. Benary, R. Labouvie, D. A. Zezyulin, V. V. Konotop, and H. Ott, Coherent perfect absorption of nonlinear matter waves, Sci. Adv. **4**, eaat6539 (2018).
[5] A. N. Vetlugin, Coherent perfect absorption of quantum light, Phys. Rev. A **104**, 013716 (2021).
[6] G. Trainiti, Y. Ra'di, M. Ruzzene, and A. Alù, Coherent virtual absorption of elastodynamic waves, Sci. Adv. **5**, eaaw3255 (2019).
[7] S. Kim, Y.-G. Peng, S. Yves, and A. Alù, Loss compensation and superresolution in metamaterials with excitations at complex frequencies, Phys. Rev. X **13**, 041024 (2023).
[8] H. J. Kimble, The quantum internet, Nature (London) **453**, 1023 (2008).
[9] T. E. Northup and R. Blatt, Quantum information transfer using photons, Nat. Photon. **8**, 356 (2014).
[10] C. Monroe, R. Raussendorf, A. Ruthven, K. R. Brown, P. Maunz, L.-M. Duan, and J. Kim, Large-scale modular quantum-computer architecture with atomic memory and photonic interconnects, Phys. Rev. A **89**, 022317 (2014).
[11] L. Jiang, J. M. Taylor, A. S. Sørensen, and M. D. Lukin, Distributed quantum computation based on small quantum registers, Phys. Rev. A **76**, 062323 (2007).
[12] L.-M. Duan, M. D. Lukin, J. I. Cirac, and P. Zoller, Long-distance quantum communication with atomic ensembles and linear optics, Nature (London) **414**, 413 (2001).
[13] L. Childress, J. M. Taylor, A. S. Sørensen, and M. D. Lukin, Fault-tolerant quantum communication based on solid-state photon emitters, Phys. Rev. Lett. **96**, 070504 (2006).
[14] J. I. Cirac, P. Zoller, H. J. Kimble, and H. Mabuchi, Quantum state transfer and entanglement distribution among distant nodes in a quantum network, Phys. Rev. Lett. **78**, 3221 (1997).
[15] E. Flurin, N. Roch, J. D. Pillet, F. Mallet, and B. Huard, Superconducting quantum node for entanglement and storage of microwave radiation, Phys. Rev. Lett. **114**, 090503 (2015).
[16] Y. Yin, Y. Chen, D. Sank, P. J. J. O'Malley, T. C. White, R. Barends, J. Kelly, E. Lucero, M. Mariantoni, A. Megrant, C. Neill, A. Vainsencher, J. Wenner, A. N. Korotkov, A. N. Cleland, and J. M. Martinis, Catch and release of microwave photon states, Phys. Rev. Lett. **110**, 107001 (2013).
[17] S. Ritter, C. Nölleke, C. Hahn, A. Reiserer, A. Neuzner, M. Uphoff, M. Mücke, E. Figueroa, J. Bochmann, and G. Rempe, An elementary quantum network of single atoms in optical cavities, Nature (London) **484**, 195 (2012).
[18] P. Goy, J. M. Raimond, M. Gross, and S. Haroche, Observation of cavity-enhanced single-atom spontaneous emission, Phys. Rev. Lett. **50**, 1903 (1983).
[19] E. Albertinale, L. Balembois, E. Billaud, V. Ranjan, D. Flanigan, T. Schenkel, D. Estève, D. Vion, P. Bertet, and E. Flurin, Detecting spins by their fluorescence with a microwave photon counter, Nature (London) **600**, 434 (2021).
[20] Z. Wang, L. Balembois, M. Rančić, E. Billaud, M. Le Dantec, A. Ferrier, P. Goldner, S. Bertaina, T. Chanelière, D. Esteve, D. Vion, P. Bertet, and E. Flurin, Single-electron spin resonance detection by microwave photon counting, Nature (London) **619**, 276 (2023).
[21] T. M. Graham, Y. Song, J. Scott, C. Poole, L. Phuttitarn, K. Jooya, P. Eichler, X. Jiang, A. Marra, B. Grinkemeyer *et al.*, Multi-qubit entanglement and algorithms on a neutral-atom quantum computer, Nature (London) **604**, 457 (2022).
[22] A. Browaeys and T. Lahaye, Many-body physics with individually controlled Rydberg atoms, Nat. Phys. **16**, 132 (2020).
[23] R. H. Hadfield, Single-photon detectors for optical quantum information applications, Nat. Photon. **3**, 696 (2009).
[24] R. Lescanne, S. Deléglise, E. Albertinale, U. Réglade, T. Capelle, E. Ivanov, T. Jacqmin, Z. Leghtas, and E. Flurin, Irreversible qubit-photon coupling for the detection of itinerant microwave photons, Phys. Rev. X **10**, 021038 (2020).
[25] J. Wenner, Y. Yin, Y. Chen, R. Barends, B. Chiaro, E. Jeffrey, J. Kelly, A. Megrant, J. Y. Mutus, C. Neill, P. J. J. O'Malley, P. Roushan, D. Sank, A. Vainsencher, T. C. White, A. N. Korotkov, A. N. Cleland, and J. M. Martinis, Catching time-reversed microwave coherent state photons with 99.4% absorption efficiency, Phys. Rev. Lett. **112**, 210501 (2014).
[26] T. A. Palomaki, J. W. Harlow, J. D. Teufel, R. W. Simmonds, and K. W. Lehnert, Coherent state transfer between itinerant microwave fields and a mechanical oscillator, Nature (London) **495**, 210 (2013).

[27] W.-J. Lin, Y. Lu, P. Y. Wen, Y.-T. Cheng, C.-P. Lee, K. T. Lin, K. H. Chiang, M. C. Hsieh, C.-Y. Chen, C.-H. Chien, J. J. Lin, J.-C. Chen, Y. H. Lin, C.-S. Chuu, F. Nori, A. F. Kockum, G. D. Lin, P. Delsing, and I.-C. Hoi, Deterministic loading of microwaves onto an artificial atom using a time-reversed waveform, Nano Lett. **22**, 8137 (2022).

[28] M. Bader, S. Heugel, A. L. Chekhov, M. Sondermann, and G. Leuchs, Efficient coupling to an optical resonator by exploiting time-reversal symmetry, New J. Phys. **15**, 123008 (2013).

[29] C. Liu, Y. Sun, L. Zhao, S. Zhang, M. M. T. Loy, and S. Du, Efficiently loading a single photon into a single-sided Fabry-Perot cavity, Phys. Rev. Lett. **113**, 133601 (2014).

[30] M. Khanahmadi, M. M. Lund, K. Mølmer, and G. Johansson, Multimode character of quantum states released from a superconducting cavity, Phys. Rev. Res. **5**, 043071 (2023).

[31] A. N. Korotkov, Flying microwave qubits with nearly perfect transfer efficiency, Phys. Rev. B **84**, 014510 (2011).

[32] E. A. Sete, E. Mlinar, and A. N. Korotkov, Robust quantum state transfer using tunable couplers, Phys. Rev. B **91**, 144509 (2015).

[33] P. Kurpiers, P. Magnard, T. Walter, B. Royer, M. Pechal, J. Heinsoo, Y. Salathé, A. Akin, S. Storz, J.-C. Besse, S. Gasparinetti, A. Blais, and A. Wallraff, Deterministic quantum state transfer and remote entanglement using microwave photons, Nature (London) **558**, 264 (2018).

[34] C. J. Axline, L. D. Burkhart, W. Pfaff, M. Zhang, K. Chou, P. Campagne-Ibarcq, P. Reinhold, L. Frunzio, S. M. Girvin, L. Jiang, M. H. Devoret, and R. J. Schoelkopf, On-demand quantum state transfer and entanglement between remote microwave cavity memories, Nat. Phys. **14**, 705 (2018).

[35] P. Campagne-Ibarcq, E. Zalys-Geller, A. Narla, S. Shankar, P. Reinhold, L. Burkhart, C. Axline, W. Pfaff, L. Frunzio, R. J. Schoelkopf, and M. H. Devoret, Deterministic remote entanglement of superconducting circuits through microwave two-photon transitions, Phys. Rev. Lett. **120**, 200501 (2018).

[36] S. J. Srinivasan, N. M. Sundaresan, D. Sadri, Y. Liu, J. M. Gambetta, T. Yu, S. M. Girvin, and A. A. Houck, Time-reversal symmetrization of spontaneous emission for quantum state transfer, Phys. Rev. A **89**, 033857 (2014).

[37] M. Pierre, I.-M. Svensson, S. R. Sathyamoorthy, G. Johansson, and P. Delsing, Storage and on-demand release of microwaves using superconducting resonators with tunable coupling, Appl. Phys. Lett. **104**, 232604 (2014).

[38] W. Pfaff, C. J. Axline, L. D. Burkhart, U. Vool, P. Reinhold, L. Frunzio, L. Jiang, M. H. Devoret, and R. J. Schoelkopf, Controlled release of multiphoton quantum states from a microwave cavity memory, Nat. Phys. **13**, 882 (2017).

[39] M. Pechal, L. Huthmacher, C. Eichler, S. Zeytinoğlu, A. A. Abdumalikov, S. Berger, A. Wallraff, and S. Filipp, Microwave-controlled generation of shaped single photons in circuit quantum electrodynamics, Phys. Rev. X **4**, 041010 (2014).

[40] Y. Mazor, M. Cotrufo, and A. Alù, Unitary excitation transfer between coupled cavities using temporal switching, Phys. Rev. Lett. **127**, 013902 (2021).

[41] A. A. Houck, D. I. Schuster, J. M. Gambetta, J. A. Schreier, B. R. Johnson, J. M. Chow, L. Frunzio, J. Majer, M. H. Devoret, S. M. Girvin, and R. J. Schoelkopf, Generating single microwave photons in a circuit, Nature (London) **449**, 328 (2007).

[42] W. F. Kindel, M. D. Schroer, and K. W. Lehnert, Generation and efficient measurement of single photons from fixed-frequency superconducting qubits, Phys. Rev. A **93**, 033817 (2016).

[43] S. Heugel, A. S. Villar, M. Sondermann, U. Peschel, and G. Leuchs, On the analogy between a single atom and an optical resonator, Laser Phys. **20**, 100 (2010).

[44] C. M. Bender and S. Boettcher, Real spectra in non-Hermitian Hamiltonians having $\mathcal{PT}$ symmetry, Phys. Rev. Lett. **80**, 5243 (1998).

[45] K. G. Makris, R. E. Ganainy, D. N. Christodoulides, and Z. H. Musslimani, Beam dynamics in $\mathcal{PT}$-symmetric optical lattices, Phys. Rev. Lett. **100**, 103904 (2008).

[46] N. Moiseyev, *Non-Hermitian Quantum Mechanics* (Cambridge University Press, Cambridge, U.K., 2011).

[47] M.-A. Miri and A. Alù, Exceptional points in optics and photonics, Science **363**, eaar7709 (2019).

[48] C. E. Rüter, K. G. Makris, R. El-Ganainy, D. N. Christodoulides, M. Segev, and D. Kip, Observation of parity–time symmetry in optics, Nat. Phys. **6**, 192 (2010).

[49] W. R. Sweeney, C. W. Hsu, S. Rotter, and A. D. Stone, Perfectly absorbing exceptional points and chiral absorbers, Phys. Rev. Lett. **122**, 093901 (2019).

[50] C. Wang, W. R. Sweeney, A. D. Stone, and L. Yang, Coherent perfect absorption at an exceptional point, Science **373**, 1261 (2021).

[51] A. Mekawy, A. Farhi, D. Stone, and A. Alù, Observation of absorbing exceptional points in the time domain (unpublished).

[52] D. M. Pozar, *Microwave Engineering* (Wiley, Hoboken, NJ, 2011).

[53] C. Leroux, A. D. Paolo, and A. Blais, Superconducting coupler with exponentially large on:off ratio, Phys. Rev. Appl. **16**, 064062 (2021).

[54] C. Lledó, R. Dassonneville, A. Moulinas, J. Cohen, R. Shillito, A. Bienfait, B. Huard, and A. Blais, Cloaking a qubit in a cavity, Nat. Commun. **14**, 6313 (2023).

[55] N. Engheta, A. Salandrino, and A. Alu, Circuit elements at optical frequencies: Nanoinductors, nanocapacitors, and nanoresistors, Phys. Rev. Lett. **95**, 095504 (2005).

[56] N. Engheta, Circuits with light at nanoscales: Optical nanocircuits inspired by metamaterials, Science **317**, 1698 (2007).

[57] A. Alù and N. Engheta, Tuning the scattering response of optical nanoantennas with nanocircuit loads, Nat. Photon. **2**, 307 (2008).

[58] M. Schnell, A. García-Etxarri, A. J. Huber, K. Crozier, J. Aizpurua, and R. Hillenbrand, Controlling the near-field oscillations of loaded plasmonic nanoantennas, Nat. Photon. **3**, 287 (2009).

[59] Y. Yao, M. A. Kats, P. Genevet, N. Yu, Y. Song, J. Kong, and F. Capasso, Broad electrical tuning of graphene-loaded plasmonic antennas, Nano Lett. **13**, 1257 (2013).

[60] N. Liu, F. Wen, Y. Zhao, Y. Wang, P. Nordlander, N. J. Halas, and A. Alù, Individual nanoantennas loaded with three-dimensional optical nanocircuits, Nano Lett. **13**, 142 (2013).

[61] H. Aouani, M. Rahmani, M. Navarro-Cía, and S. A. Maier, Third-harmonic-upconversion enhancement from a single semi-

conductor nanoparticle coupled to a plasmonic antenna, Nat. Nanotechnol. **9**, 290 (2014).

[62] V. Venkataraman, K. Saha, P. Londero, and A. L. Gaeta, Few-photon all-optical modulation in a photonic band-gap fiber, Phys. Rev. Lett. **107**, 193902 (2011).

[63] M. Ren, B. Jia, J.-Y. Ou, E. Plum, J. Zhang, K. F. MacDonald, A. E. Nikolaenko, J. Xu, M. Gu, and N. I. Zheludev, Nanostructured plasmonic medium for terahertz bandwidth all-optical switching, Adv. Mater. **23**, 5540 (2011).

[64] See Supplemental Material at http://link.aps.org/supplemental/10.1103/PhysRevA.109.L041502 for a detailed calculation of the EP, calculation of another EP, calculation of the scattered field for an input of the form $e^{i\omega t-\Gamma t}$, and an explanation on how to tune a CCD system to an EP in the lossy and lossless cases.